

Applicability of the QMD model to various nuclear reactions

Koji Niita

RIST (Research Organization for Information & Technology), Tokai, Ibaraki, Japan

Abstract

The basic formulation and the detail of the parameters included in the standard QMD model, JQMD (JAERI Quantum Molecular Dynamics) are described. Various cross sections calculated by the QMD model are compared with the data at various energies for heavy ion reactions and also nucleon induced reactions. The range of the applicability of the QMD model and the limitation of the QMD model are discussed.

1 Introduction

The cross sections of intermediate and high energy nuclear reactions are strongly required in design study of many facilities such as accelerator-driven systems, intense pulse spallation neutron sources, and also in medical and space technology. There is, however, few evaluated nuclear data of intermediate and high energy nuclear reactions. Therefore, we have to use reaction models or systematics to obtain the cross sections, which are essential ingredients of high energy particle transport code to estimate neutron yield, heat deposition and many other quantities of the transport phenomena in materials.

In the particle and heavy ion transport code system PHITS [1], we have used two simulation codes JAM [2] (Jet AA Microscopic Transport Model) and JQMD [3] (JAERI Quantum Molecular Dynamics) to describe the intermediate and high energy nuclear reactions. JAM is a simulation code based on INC (intra-nuclear cascade) model, which explicitly treats all established hadronic states including resonances with explicit spin and isospin as well as their anti-particles. We have parametrized all hadron-hadron cross sections based on the resonance model and string model by fitting the available experimental data. On the other hand, JQMD is a simulation code based on the molecular dynamics. A typical feature of QMD compared with that of the INC model is that QMD can describe not only nucleon-nucleus reactions but also nucleus-nucleus reactions in the same framework. The QMD model has been widely used to analyze various aspects of heavy ion reactions as well as of nucleon-induced reactions [3,4], and has shed light on several exciting topics in heavy ion physics, for example, the multifragmentation, the flow of the nuclear matter, and the energetic particle production [5].

In this paper, we describe the basic formulation and the detail of the parameters included in the JQMD code, and we show various cross sections calculated by the JQMD code compared with the data at various energies for heavy ion reactions and also nucleon induced reactions. Next we summarize the recent extensions of the JQMD code. Finally, we discuss the range of the applicability of the QMD model and the limitation of the QMD model.

2 Basic formulation of JQMD

The QMD method is a semi-classical simulation method in which each nucleon state (denoted by a subscript i) is represented by a Gaussian wave packet. The total wave function is assumed to be a direct product of these wave functions. Thus the one-body distribution function is obtained by the Wigner transform of the wave function,

$$f_i(\vec{r}, \vec{p}) = 8 \cdot \exp\left[-\frac{(\vec{r} - \vec{R}_i)^2}{2L} - \frac{2L(\vec{p} - \vec{P}_i)^2}{\hbar_2}\right], \quad (1)$$

where L is a parameter representing the spatial spread of a wave packet, \vec{R}_i and \vec{P}_i corresponding to the centers of a wave packet in the coordinate and momentum space, respectively. The equation of motion of \vec{R}_i and \vec{P}_i is given, on the basis of the time-dependent variational principle, by the Newtonian equations:

$$\dot{\vec{R}}_i = \frac{\partial H}{\partial \vec{P}_i}, \quad \dot{\vec{P}}_i = -\frac{\partial H}{\partial \vec{R}_i}, \quad (2)$$

and the stochastic N-N collision term [3]. We have adopted the Hamiltonian H consisting of the relativistic energy and the Skyrme-type effective N-N interaction plus Coulomb and symmetry energy terms:

$$\begin{aligned} H = & \sum_i \sqrt{m_i^2 + \vec{P}_i^2} \\ & + \frac{1}{2} \frac{A}{\rho_0} \sum_i \langle \rho_i \rangle + \frac{1}{1+\tau} \frac{B}{\rho_0^\tau} \sum_i \langle \rho_i \rangle^\tau \\ & + \frac{1}{2} \sum_{i,j(\neq i)} \frac{e_i e_j}{|\vec{R}_i - \vec{R}_j|} \text{erf}\left(|\vec{R}_i - \vec{R}_j| / \sqrt{4L}\right) \\ & + \frac{C_s}{2\rho_0} \sum_{i,j(\neq i)} c_i c_j \rho_{ij}, \end{aligned} \quad (3)$$

where ‘‘erf’’ denotes the error function, the e_i is the charge of the i -th particle, and the c_i is 1 for proton, -1 for neutron and 0 for the other particles. With the definition

$$\begin{aligned} \rho_i(\vec{r}) & \equiv \int \frac{d\vec{p}}{(2\pi\hbar)^3} f_i(\vec{r}, \vec{p}) \\ & = (2\pi L)^{-3/2} \exp\left[-(\vec{r} - \vec{R}_i)^2 / 2L\right] \end{aligned} \quad (4)$$

the other symbols in Eq.(3) are given as:

$$\begin{aligned} \langle \rho_i \rangle & \equiv \sum_{j \neq i} \rho_{ij} \equiv \sum_{j \neq i} \int d\vec{r} \rho_i(\vec{r}) \rho_j(\vec{r}) \\ & = \sum_{j \neq i} (4\pi L)^{-3/2} \exp\left[-(\vec{R}_i - \vec{R}_j) / 4L\right] \end{aligned} \quad (5)$$

The symmetry energy coefficient C_s is taken to be 25 MeV. The four remaining parameters, the saturation density ρ_0 , the Skyrme parameters A , B and τ are chosen to be 0.168 fm^{-3} , -124 MeV, 70.5 MeV and $4/3$, respectively. These values give the binding energy/nucleon of 16 MeV at the saturation density ρ_0 and the compressibility of 237.7 MeV (soft EOS) for nuclear matter limit. The only arbitrary parameter in QMD is the width parameter L , which is fixed to be 2 fm^2 to give stable ground states of target nuclei in a wide mass range.

In addition to the Newtonian equation Eq.(2), the time evolution of the system is affected by the two-body collision term. In the QMD model, the stochastic two-body collision process is described in the same method as in the intra-nuclear cascade model except for the Pauli blocking factor. The final blocking probability is determined by $[1 - f(\vec{r}, \vec{p}, t)]$ which is obtained by summing up the each one-body distribution function given by Eq.(1).

The ground state of the target and/or projectile is generated by packing \vec{R}_i and \vec{P}_i randomly based on the Woods-Saxon type distribution in the coordinate space and corresponding local Thomas-Fermi approximation in the momentum space, seeking a configuration to reproduce the binding energy included in the nuclear data table within a certain uncertainty. The ground state obtained by

this procedure is a self-bind system and rather stable up to the time 200 fm/c, which is enough time for the dynamical stage of the reaction.

The QMD simulation, as well as the JAM simulation, describes the dynamical stage of the reactions. At the end of the dynamical stage, excited nuclei are created and must be forced to decay in a statistical way to get the final observed state. In PHITS, the GEM [6] model is employed for light particle evaporation and fission process of the excited residual nucleus. The switching time, when we switch the QMD calculation to GEM, is an arbitrary parameter in the model. We have checked the dependence of the final results on the switching time and found that the final results are not sensitive to the switching time if we use the switching time from 100 fm/c to 150 fm/c for nucleon-induced reactions [3].

3 Comparisons with the experimental data

3.1 Results of nucleon-induced reactions

We have applied the JQMD code intensively to nucleon-nucleus reactions and checked its validity [3,4]. First we show the results of the JQMD code for the particle spectra emitted from proton induced reactions. Fig. 1 shows the neutron energy spectra for the reaction $p + {}^{208}\text{Pb}$ at 256 MeV [7] and 3 GeV [8]. The JQMD results of the neutron energy spectra agree well with the data from 1 MeV up to the beam energy.

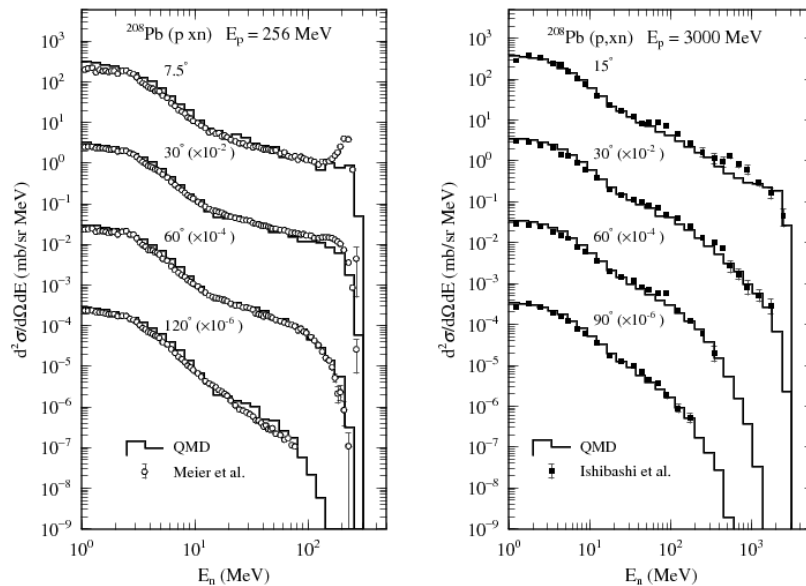


Fig.1: Neutron energy spectra for the reaction $p + {}^{208}\text{Pb}$ at different laboratory angles as indicated in the figure. The incident energy is 256 MeV (left-hand-side) and 3 GeV (right-hand side). The solid histograms are the results of QMD and the open circles and the full boxes with error bars denote the experimental data taken from refs.[7,8].

In Fig. 2 we plot the invariant cross sections of the proton (left-hand-side) and negative pion (right-hand-side) emission for the reaction $p (3.17 \text{ GeV}) + {}^{27}\text{Al}$ [9]. These figures indicate the JQMD code can reproduce quit well the overall features of the outgoing protons and pions as well as neutrons without assuming any reaction mechanism, and without changing the parameter set.

Next we have analyzed the fragment production from the proton induced reaction. In Fig.3, we show the production cross sections of various fragments for $p (1.5 \text{ GeV}) + {}^{56}\text{Fe}$ reaction [10]. It is clearly concluded that the JQMD code reproduces well the fragment production cross sections in the

whole mass region, including the light clusters such as α and intermediate mass fragments (IMF) ($A \sim 20$ to 30) except for ${}^7\text{Be}$ where the results of JQMD underestimate the data by approximately 2 order of magnitude.

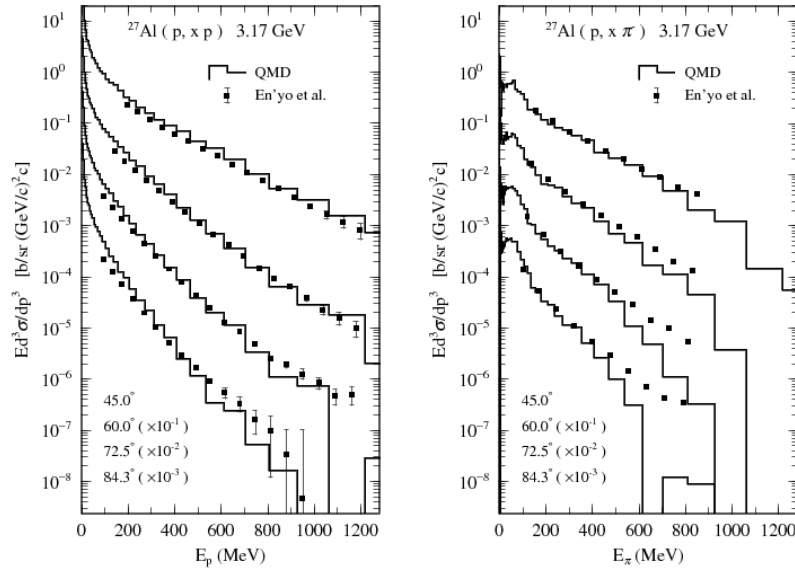


Fig. 2: Invariant cross sections of the proton (left-hand-side) and negative pion (right-hand-side) emission for the reaction p (3.17 GeV) + ${}^{27}\text{Al}$ at different laboratory angles as indicated in the figure. Full boxes with error bars are the experimental data taken from ref.[9] and the results of QMD are denoted by solid histograms.

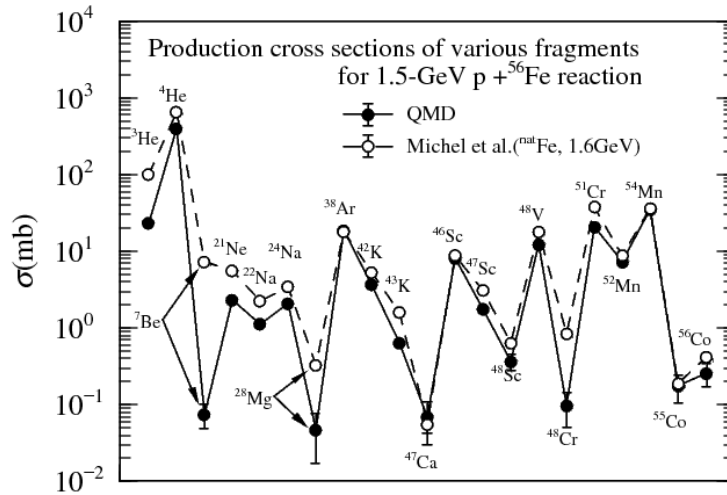


Fig.3: Production cross sections of various fragments for p (1.5 GeV) + ${}^{56}\text{Fe}$ reaction. The full circles connected by a solid line denote the results of QMD, while the open circles connected by a dashed line are obtained experimentally by Michel et al. measured at 1.6 GeV for ${}^{\text{nat}}\text{Fe}$ [10].

3.2 Results of heavy-ion reactions

So far the QMD model has shed light on several exciting topics in heavy-ion physics, e.g. the multi-fragmentation, the flow of the nuclear matter, and the energetic particle productions [11]. Here we show two examples of the basic observables from heavy-ion reactions calculated by the JQMD code.

In Fig.4(a) we represent the results of π^- energy spectra for the reaction $^{12}\text{C} + ^{12}\text{C}$ at 800 MeV/nucleon. The result of JQMD reproduces the experimental data [12]. We notice that this calculation has been done in the same formulation and also with the same parameter set as used in the nucleon-induced reactions.

Next example is the neutron energy spectra from the reaction $^{12}\text{C} + ^{208}\text{Pb}$ at 400 MeV/nucleon, which is shown in Fig.4(b). The neutron produced in heavy-ion reactions is very important in the shielding design of new facilities because of its large attenuation length in shielding materials. Recently, secondary neutrons from heavy-ion reactions have been systematically measured using thin and thick targets by HIMAC of NIRS (National Institute of Radiological Sciences), Japan [13,14]. Fig.4(b) shows that the QMD code roughly reproduced the measured cross sections for the C beams.

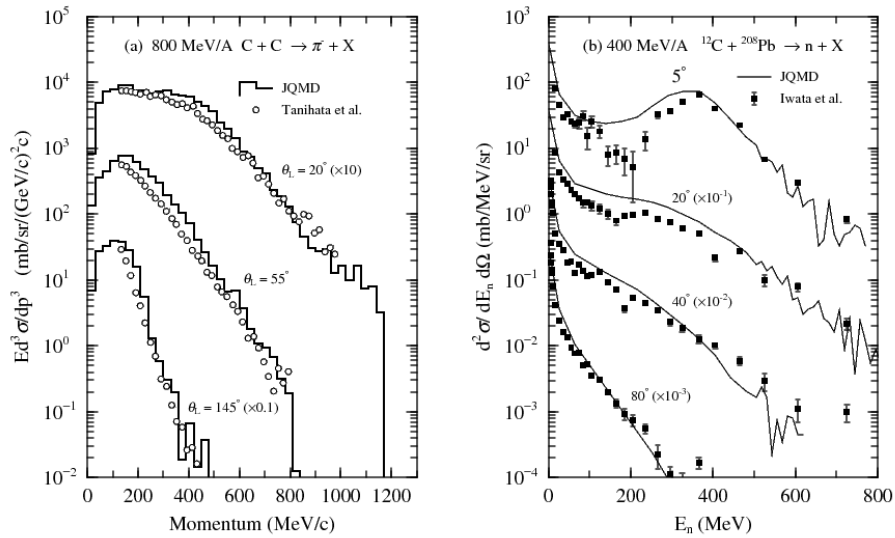


Fig.4: (a) (left panel) π^- energy spectra for the reaction ^{12}C (800 MeV/nucleon) + ^{12}C and (b) (right panel) neutron energy spectra for the reaction ^{12}C (400 MeV/nucleon) + ^{208}Pb at different laboratory angles as indicated in the figure. The solid histograms and the solid lines are the results of the QMD and the open circles and solid squares denote the experimental data taken from ref.[12,13].

4 Extensions of the JQMD code

4.1 Low energy heavy ion reactions

One of arbitrary parameters in the JQMD code is the switching time, when we switch the QMD calculation to GEM, as mentioned before. We have checked the dependence of the final results on the switching time for nucleon-induced reactions at 1.5 GeV [3], and fixed it as 150 fm/c. Recently, we have analyzed low energy heavy ion reactions and checked the sensitivity of the switching time [15]. Fig. 5 shows the neutron energy spectrum at 90 degree in the laboratory system from thick Cu target bombarded 10 MeV/u ^{12}C beam. We have changed the switching time from 50 fm/c to 150 fm/c in the calculations and compared with the experimental data [16]. From this figure, we conclude that the switching time value 100 fm/c is the best value to simulate the neutron energy spectra from the low energy heavy ion reactions. This value, however, does not affect so much the previous results with the value of switching time 150 fm/c for nucleon induced reactions and heavy ion reactions at much higher energy, since they are very stable if we use the switching time from 100 fm/c to 150 fm/c.

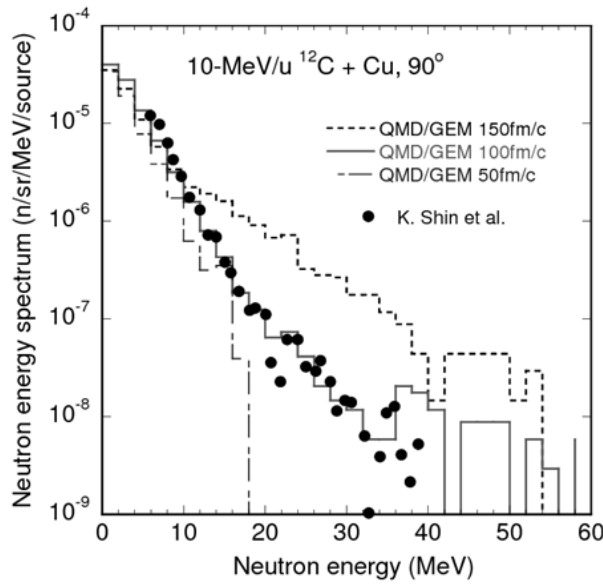


Fig.5: Neutron energy spectrum at 90 degree in the laboratory system from thick Cu target bombarded 10 MeV/u ^{12}C beam. The filled squares are the experimental data [16], while the dashed (150 fm/c), full (100 fm/c) and dot-dashed (50 fm/c) lines present the JQMD+GEM results by changing the switching time.

4.2 High energy extension of the JQMD model

The JQMD code was developed with the intent to provide a unified description of various aspects of nuclear reactions. By combining JQMD and the statistical decay model GEM, one obtains a hybrid model that can describe accurately both the fast dynamical stage and the slow statistical stage of the reaction and, thus, reproduce measured double-differential cross sections for the production of protons and neutrons in proton-nucleus [3,4] and nucleus-nucleus collisions [13,14]. There are other observables, however, that does not reproduce as accurately as double-differential cross sections for nucleon production; for example, fragment yields in heavy-ion reactions are sometimes in sensible discrepancy with the experimental data [17], especially for soft, peripheral reactions that only entail stripping of a small number of nucleons. The cause of these shortcomings can be traced back to a small intrinsic instability of the ground state of the JQMD nucleus, which in fact can emit nucleons spontaneously because of potential-energy fluctuations and alter significantly the final yields of soft, peripheral reactions (hard, central collisions are not very sensitive to the details of the initial configuration).

These instabilities have two main reasons: firstly, the JQMD formalism is not completely relativistically covariant, which implies that the dynamics of a nucleus is somehow dependent on the frame of reference used. Secondly, the ground state that JQMD nuclei are initialized in is only an approximation; in all QMD models, it is conceptually impossible to create the "real" ground state, i.e. the lowest-energy eigenstate of the quantum-mechanical n-body Hamiltonian operator, which is influenced by Pauli's exclusion principle. (In a semi-classical n-body theory, like QMD-models, Pauli's principle is not taken into account and particles are thus allowed to move closer to each other). If we want to describe peripheral nucleus-nucleus reactions consistently in the JQMD framework, it is necessary to switch to a relativistically covariant formalism and to improve the ground-state initialization algorithm, in order to suppress spurious potential-energy fluctuations and particle decays. Recently, Mancusi et al. has thus introduced R-JQMD [18], an improved and fully covariant version of JQMD that also features a new ground-state initialization algorithm for nuclei. This new version of

JQMD is expected to give much reliable results for the fragmentation cross sections at high energy heavy-ion reactions. However, the double differential cross sections of neutron from proton induced reactions, for an example, are not as sensitive to relativistic effects, thus, one should not expect large differences in the results by R-JQMD and JQMD. We have verified this by computing double differential energy angle cross sections in Fig. 6. It is clear that R-JQMD and JQMD do not differ very much as far as neutrons spectra are concerned [18].

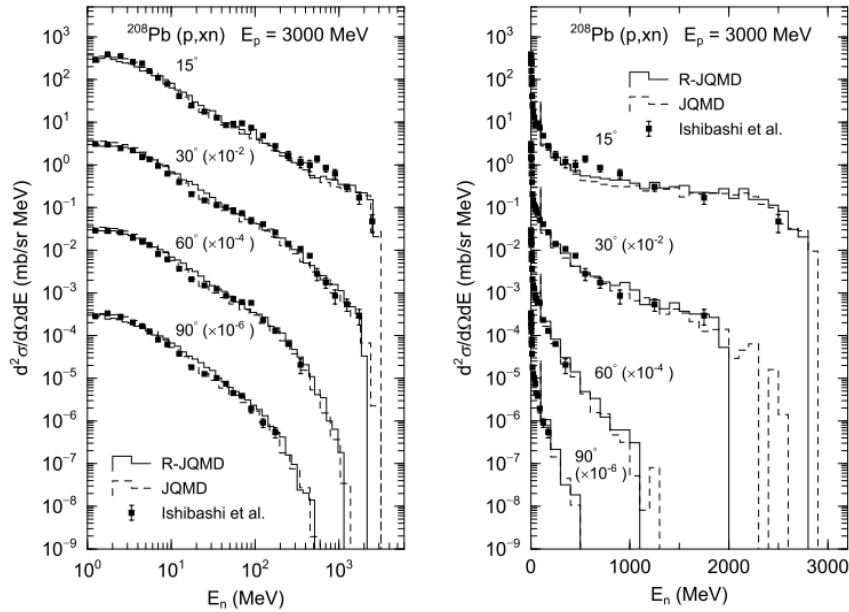


Fig. 6: Double-differential energy-angle cross sections for the production of neutrons in the reaction between 3-GeV protons and lead, with data taken from [19]. Left: log scale; right: linear scale. No significant difference can be observed between JQMD and R-JQMD.

5 Conclusions

We have described the basic formulation and the detail of the parameters included in the JQMD code and shown the various cross sections calculated by the JQMD code for various nuclear reactions, nucleon-induced reaction and heavy ion reactions from low energy around 10 MeV/u up to several hundreds GeV/u. It should be noticed that the results of the JQMD code reproduced these experimental data very well with the same parameter set. For very low energy heavy ion reactions around 10 MeV/u, we have checked the dependence of the results on the switching time from JQMD to GEM, and found 100 fm/c is a suitable value for the switching time. This value is within the range of the switching time which we have previously estimated for nucleon induced reactions. For relativistic high energy heavy ion reactions, we have introduced a fully covariant version of JQMD, R-JQMD, which suppresses spurious potential-energy fluctuations and particle decays caused by non-covariant treatment of the dynamics. However, there are some observables which the present JQMD model does not reproduce well. One is an observable related to the discrete levels near the ground state, and another is related to coherent phenomena such as multi-fragmentations. In spite of these problems, there are two reasons that we should develop the QMD model further. First, many simulation codes based on the intra-nuclear cascade and evaporation model have been developed with including new parameters and ingredients. However, most of them are not designed to treat nucleus-nucleus collisions. Second, the improvement of the QMD model is focused on that of the effective interactions, which is closely related to the fundamental nuclear physics [20]. This is a very nice opportunity for the collaboration of the fundamental nuclear physics and the application field.

References

- [1] H. Iwase, K. Niita and T. Nakamura, J. Nucl. Sci. Technol. **39** (2002) 1142; K. Niita, T. Sato, H. Iwase, H. Nose, H. Nakashima, L. Sihver, Radiat. Meas. **41** (2006) 1080.
- [2] Y. Nara, N. Otuka, A. Ohnishi, K. Niita and S. Chiba, Phys. Rev. **C61** (2000) 024901.
- [3] K. Niita, S. Chiba, Toshiki Maruyama, Tomoyuki Maruyama, H. Takada, T. Fukahori, Y. Nakahara, A. Iwamoto, Phys. Rev. **C52** (1995) 2620.
- [4] S. Chiba, O. Iwamoto, T. Fukahori, K. Niita, Toshiki Maruyama, Tomoyuki Maruyama, A. Iwamoto, Phys. Rev., **C54** (1996) 285, S. Chiba, M.B. Chadwick, K. Niita, Toshiki Maruyama, Tomoyuki Maruyama, A. Iwamoto, Phys. Rev., **C53** (1996) 1824.
- [5] J. Aichelin, Phys. Rep. **202** (1991) 233.
- [6] S. Furihata, Nucl. Instr. and Meth. **B171** (2000) 251.
- [7] W. B. Amian, B. C. Byrd, C. A. Goulding, M. M. Meier, G. L. Morgan, C. E. Moss, and D. A. Clark, Nucl. Sci. and Eng., **112** (1992) 78.
- [8] K. Ishibashi, et al., J. Nucl. Sci. Technol., **32** (1995) 827.
- [9] H. En'yo, et al., Phys. Lett., **B159** (1985) 1.
- [10] R. Michel, et al., Nucl. Instr. and Meth., **B103** (1995) 183.
- [11] W. Cassing, V. Metag, U. Mosel, K. Niita, Phys. Rep. **188** (1990) 363.
- [12] I. Tanihata et al., Phys. Lett., **B87** (1979) 349.
- [13] Y. Iwata et al., Phys. Rev., **C64** (2001) 054609.
- [14] T. Kurosawa, et al., Nucl. Sci. and Eng., **132** (1999) 30; Journal of Nucl. Sci. and Technol. **36-1**, (1999) 42; Nucl. Instr. and Meth. **A430** (1999) 400; Phys. Rev. **C62** (2000) 044615.
- [15] Y. Iwamoto, R.M.Ronningen, K. Niita, the 2009 Particle Accelerator Conference, Vancouver, Canada, TU6RFP058.
- [16] K. Shin, et al., Nucl. Sci. Eng. **120** (1995) 40.
- [17] L. Sihver, et al., Adv. Space Res. **40** (2007) 1320.
- [18] Davide Mancusi, Koji Niita, Tomoyuki Maruyama, Lembit Sihver, Phys. Rev. **C79**, (2009) 014614.
- [19] Ishibashi, et al., J. Nucl. Sci. Technol. **34** (1997) 529.
- [20] Toshiki Maruyama, K. Niita, K. Oyamatsu, Tomoyuki Maruyama, S. Chiba, A. Iwamoto, Phys. Rev., **C57** (1998) 655.